

# Kent Academic Repository

## Full text document (pdf)

### Citation for published version

Appukutti, Nadeema and Serpell, Christopher J. (2019) Sequence Isomerism in Uniform Polyphosphoester Programmes Self-Assembly and Folding. Working paper. ChemRxiv 10.26434/chemrxiv.7666316.v1 <<https://doi.org/10.26434/chemrxiv.7666316.v1>>.

### DOI

<https://doi.org/10.26434/chemrxiv.7666316.v1>

### Link to record in KAR

<https://kar.kent.ac.uk/78376/>

### Document Version

Pre-print

#### Copyright & reuse

Content in the Kent Academic Repository is made available for research purposes. Unless otherwise stated all content is protected by copyright and in the absence of an open licence (eg Creative Commons), permissions for further reuse of content should be sought from the publisher, author or other copyright holder.

#### Versions of research

The version in the Kent Academic Repository may differ from the final published version.

Users are advised to check <http://kar.kent.ac.uk> for the status of the paper. **Users should always cite the published version of record.**

#### Enquiries

For any further enquiries regarding the licence status of this document, please contact:

[researchsupport@kent.ac.uk](mailto:researchsupport@kent.ac.uk)

If you believe this document infringes copyright then please contact the KAR admin team with the take-down information provided at <http://kar.kent.ac.uk/contact.html>

# Sequence Isomerism in Uniform Polyphosphoesters Programmes Self-Assembly and Folding

*Nadeema Appukutti and Christopher J. Serpell\**

School of Physical Sciences, Ingram Building, University of Kent, Canterbury, Kent, CT2 7NH, UK  
Email: C.J.Serpell@kent.ac.uk / Twitter: @CJSerpell

**Non-natural sequence-defined polymers have the potential to recapitulate the unique structures and functions of proteins. To achieve this goal requires not only high-efficiency synthesis platforms, but also an understanding of the relationship between sequence and folding/self-assembly. In a step towards that goal, we have here exploited the high-yielding solid phase phosphoramidite synthesis commonly used to make DNA, and generated two sequence-isomeric polymers which display sequence-programmed folding and self-assembly. These findings open up possibilities for more sophisticated sequence/structure relationships using the same synthetic platform.**

The roles of proteins and DNA are central to all known living systems. The remarkable functions they embody are determined by a common blueprint: a specific sequence of monomers in a polymer is converted into a 3D structure through supramolecular interactions; and a further level of interactions translates that structure into function. Since biological functions are still far beyond what can be performed through synthetic chemistry, recapitulating this blueprint is a major scientific goal. Accordingly, the synthesis of sequence-controlled and perfectly sequence-defined non-natural polymers is an area of enormous current interest.<sup>1-3</sup> However, studies on sequence-defined polymers focus primarily on synthesis, mainly of small oligomers (<5 kDa), and exploration of supramolecular chemistry is rare.<sup>4,5</sup> Similarly, the folding of single synthetic polymer chains into nanoparticles (single chain nanoparticles, SCNPs) is receiving much attention,<sup>6</sup> but typically uses polymers with low levels of sequence control.<sup>7</sup> Conversely, the foldamer community, approaching the problem from the small molecule perspective, seldom make macromolecular constructs,<sup>8,9</sup> and examples combining more than one folding motif are almost unknown.<sup>10</sup>

The solid phase phosphoramidite method<sup>11</sup> used routinely to create DNA strands has recently emerged as a leading strategy for creation of truly macromolecular and sequence-defined non-nucleosidic polymers. To date, this system has been employed to modify the self-assembly and biological activity of DNA itself,<sup>12-16</sup> and as a data storage medium.<sup>17-19</sup> Shorter oligomers of chromophores produced this way display both unusual self-assembly and photonic properties.<sup>20-23</sup> Polyphosphoesters with degree of polymerisation (DP) of up to 104 have been produced in this format,<sup>18</sup> demonstrating its capacity to more closely recreate the scale of biopolymer structure. At the same time, the phosphate group offers many benefits in biology,<sup>24</sup> and polyphosphoesters synthesised by more classical polymerisations themselves are emerging as new high-value polymers whose biodegradability, customisability, and flame retardancy offer opportunities in materials and healthcare.<sup>25,26</sup> However, the intrinsic supramolecular behaviour of macromolecular sequence-defined polyphosphoesters has yet to be explored.<sup>27</sup>

We herein report the supramolecular behaviour of two sequence-isomeric polyphosphoesters arising from hydrophobic/hydrophilic phenomena and electrostatic interactions. This represents a new leading example of sequence-determined self-assembly in entirely non-biological macromolecules and opens up vast possibilities for further elaboration of the sequence-defined polyphosphoester platform.

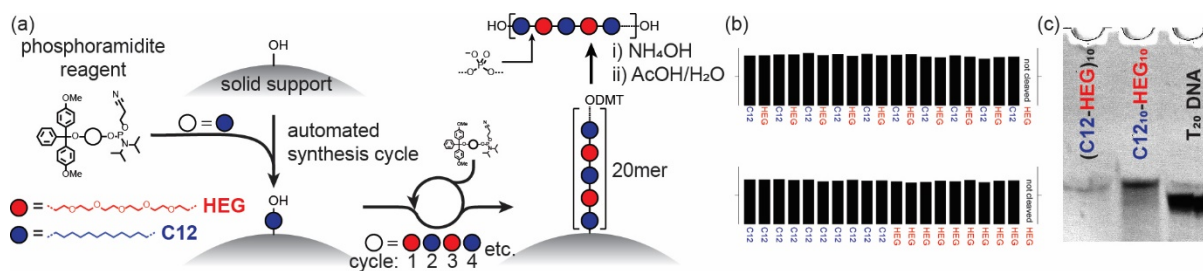


**Figure 1.** (a) Synthesis of sequence-defined polyphosphodiester. (b) Trityl histograms showing successful synthesis. (c) Denaturing polyacrylamide gel electrophoresis (20 %) showing single products in line with 20mer DNA.

We used two monomers, dodecane diol (**C12**) and hexa(ethylene glycol) (**HEG**) – these are commercially available as dimethoxytrityl (DMT)-protected phosphoramidite reagents for use as ‘spacers’ in oligonucleotide strands to either break helicity constraints or otherwise separate oligonucleotide segments from surfaces or each other. In our hands, they were used to provide a hydrophobic (**C12**) or hydrophilic (**HEG**) region within the polymers. Using an automated DNA synthesiser, we created two extremes of sequence in 20mers – a diblock arrangement **C12**<sub>10</sub>-**HEG**<sub>10</sub> and an alternating polymer (**C12-HEG**)<sub>10</sub>. Since both of the monomers are hexamers of conventional polymers, the products could be said to have a combined DP of 120 ( $M_w = 6023$  Da), with regular punctuations by phosphodiester groups. Since solid-phase synthesis has a stepwise yield of up to 95.5%, the polymer materials formed have near-perfect sequence control and negligible dispersity. The phosphates will be deprotonated all but the most acidic aqueous media, and are therefore expected to provide water solubility.

The polymers were synthesised from controlled pore glass (CPG) supports via the UnyLinker,<sup>28</sup> eliminating the first nucleobase commonly installed on CPG supports (Fig. 1a). A standard couple-cap-oxidise-deblock cycle on an automated synthesiser was employed, with the exception of an extended coupling time (10 minutes) as a precautionary measure. In-line monitoring of the outgoing DMT cation concentration by UV absorption at the deblock steps confirmed that the monomers had been successfully added all the way to the 19mer (Fig. 1b). However, due to the lack of UV-active groups in the final polymer which would enable UV quantification (as is routine for DNA), the final DMT was left on the strand. After cleavage from the support, deprotection of the phosphate groups, and clean-up *via* size exclusion chromatography, the DMT groups were cleaved using 4:1 acetic acid: water, and the UV absorbance at 500 nm measured. This intensity was compared against the absorbance of known concentrations of DMT-Cl treated similarly to obtain yields for the synthesis. These yields (1.4  $\mu\text{mol}$  and 0.59  $\mu\text{mol}$  from nominally 1  $\mu\text{mol}$  of starting functionality, subject to weighing errors) are similar to those obtained when synthesising DNA in the conventional way. Because of the handle provided by the negatively charged phosphates, gel electrophoresis was used to confirm that the synthesis had been successful (Fig. 1c). We found that in order to visualise the bands on the gel it was necessary to load a much greater quantity of the polymer (on the order of 1 nmol) onto polyacrylamide gels than would be needed for DNA (order of 10 pmol), using stains available for DNA gels (methylene blue here).

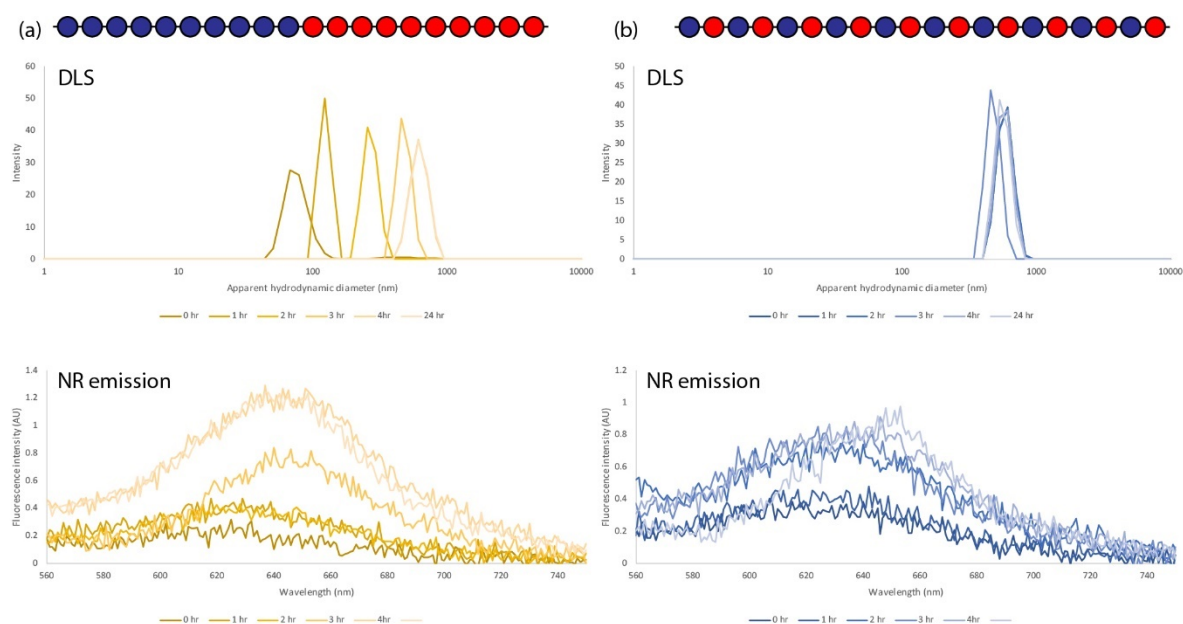


**Figure 2.** DLS (top) and NR emission measurements (bottom) on (a) **C12<sub>10</sub>-HEG<sub>10</sub>** and (b) **(C12-HEG)<sub>10</sub>** in TBE buffer at 100  $\mu$ M.

Self-assembly of the two polymers was conducted under a range of conditions to assess the effect sequence on 3D structure. Previous results on similar polymers grown from DNA strands<sup>12</sup> suggested that, as with DNA, cations such as  $Mg^{2+}$  would be required in order to permit the polymers to come together, and we anticipated that it would be similar without the oligonucleotide. Specifically, the diblock sequence **C12<sub>10</sub>-HEG<sub>10</sub>** would be expected to yield spherical micelles, whereas the alternating **(C12-HEG)<sub>10</sub>** system would be expected to show no self-assembly at all since the hydrophobic parts would fail to reach critical mass. We therefore used two buffers, tris-borate-EDTA (TBE) containing no free metals, and tris-acetate-magnesium acetate (TAMg) containing 12.5 mM  $Mg^{2+}$ . These buffers are commonly used for DNA studies under denaturing and native conditions respectively.

Assessment of self-assembly was screened using dynamic light scattering (DLS) at timed intervals for both polymers initially in TBE buffer, to give apparent hydrodynamic diameters (i.e. assuming a sphere; so numbers should be considered only semiquantitatively). Over the course of 4 hours at 100  $\mu$ M, **C12<sub>10</sub>-HEG<sub>10</sub>** increased in apparent hydrodynamic diameter from 72 nm to 615 nm, remaining at that size for the remainder of the 24 hour period of measurement (Fig. 2a); measured at 10  $\mu$ M (Fig. S1) an initial peak at 274 nm evolved gradually to 714 nm, but had returned to 255 nm after 24 hours, while at 1  $\mu$ M (Fig. S2), the apparent size fluctuated around peaks at 122 and 413 nm (although data quality was poor at this concentration). This suggests the formation of different superstructures at different concentrations. Conversely, at 100  $\mu$ M **(C12-HEG)<sub>10</sub>** produced assemblies with an apparent diameter of 615 nm from the outset which were stable over the course of the measurement (Fig. 2b). At 10  $\mu$ M (Fig. S1), the peak moved from 263 nm to 85 nm, and back to 263 nm, while at 1  $\mu$ M (Fig. S2) the scattering was too weak to analyse with confidence.

The self-assembly was examined in parallel using the fluorescent membrane probe Nile Red (NR). NR fluoresces in hydrophobic media but is negligibly emissive in water – it can therefore be used to examine the extent of the hydrophobic microenvironment formed as a result of self-assembly.<sup>29,30</sup> For **C12<sub>10</sub>-HEG<sub>10</sub>** at 100  $\mu$ M, the integrated fluorescence intensity increased over the first four hours and then remained stable for the remainder of the 24 hours (Fig. 2a). At 10 and 1  $\mu$ M (Fig. S1, S2), the intensity decreased initially before stabilising. Again, this is consistent with a change in structure with

respect to concentration. **(C12-HEG)<sub>10</sub>** also gained intensity over time at 100  $\mu\text{M}$  (Fig. 2b), but lost intensity progressively at 10  $\mu\text{M}$  (Fig. S1). At 1  $\mu\text{M}$  (Fig. S2) there was no change in the already weak signal.

The integrated fluorescence intensity arising from the block sequence sample was generally higher than that of the alternating polymer, indicating that the stretches of contiguous **C12** units provide a more significant hydrophobic microenvironment.

The effects of sequence upon self-assembly were also manifested in TAMg buffer (Fig. S3-5). As measured by DLS, the block copolymer **C12<sub>10</sub>-HEG<sub>10</sub>** at 100  $\mu\text{M}$  immediately produced assemblies with an apparent diameter of 712 nm. The overall size distribution then decreased in a non-linear way, with populations evolving at 91 nm 3-4 hours while the large peak decreased, and after 24 hours a broad distribution peaking at 295 nm was seen. At 10  $\mu\text{M}$  a stable population around 600 nm existed, and at 1  $\mu\text{M}$  over 24 hours particle size switched from around 115 nm to a sharp peak at 16 nm. The latter would be consistent with SCNPs, but again data quality was low at this level of dilution. NR emission decreased with time in this buffer at all concentrations, again changing little after the 4 hour mark, with a far greater effect seen at 100  $\mu\text{M}$  than at the lower concentrations, suggesting reorganisation of chains concomitant with the change in size. The alternating polymer **(C12-HEG)<sub>10</sub>** gave the same DLS readings as in TBE at 100  $\mu\text{M}$  – a stable population with an apparent diameter of 615 nm, while the initially weak NR fluorescence decreased to barely-measurable levels. At lower concentrations the DLS data was not of sufficient quality to be used, and the NR emission was not distinguishable from the background.

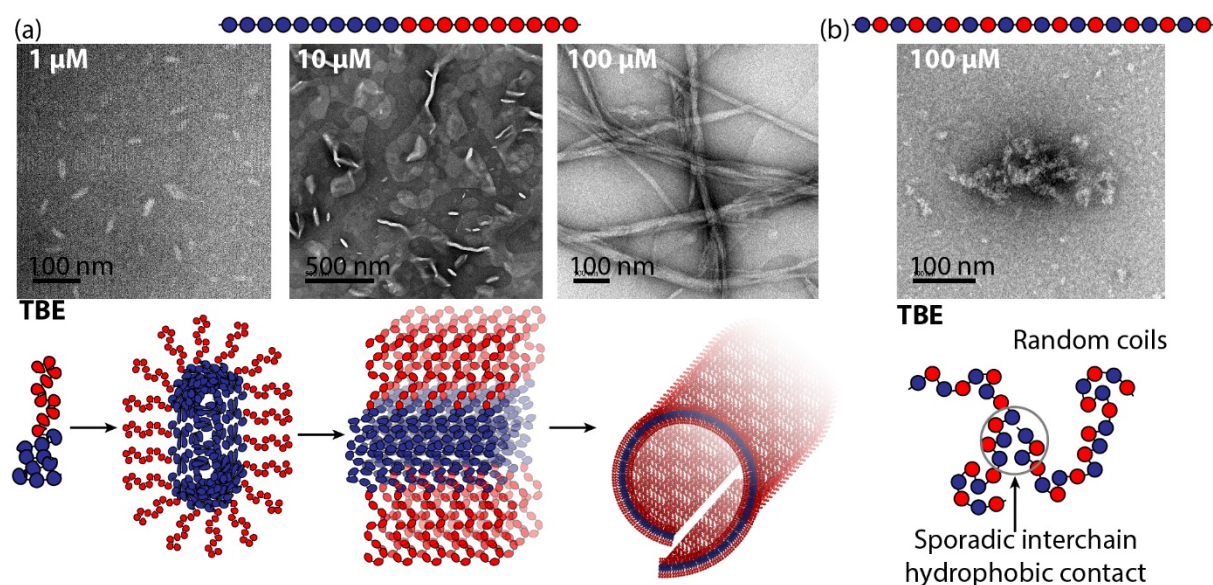


**Figure 3.** Self-assembly in TBE buffer of (a) **C12<sub>10</sub>-HEG<sub>10</sub>** and (b) **(C12-HEG)<sub>10</sub>**.

To examine the structure of the self-assembled nanomaterials, transmission electron microscopy (TEM) and atomic force microscopy (AFM) studies were conducted at three different concentrations after 24 hours of incubation in buffer before deposition. For **C12<sub>10</sub>-HEG<sub>10</sub>** assembled in TBE buffer (Fig. 3a, S6-S8), at 100  $\mu\text{M}$ , structures with widths of 10 – 40 nm, and multiple micrometers in length were observed. Features consistent with twisting (both helical directions being observed), fraying, and unrolling were seen, consistent with the fibres being formed through rolling of lamellar structures. The same structures could be seen using AFM (Fig. S12). This hypothesis was tested by depositing diluted samples and examining the self-assembly. At 10  $\mu\text{M}$ , **C12<sub>10</sub>-HEG<sub>10</sub>** was found to produce primarily lamellae which exhibited ‘pinching’ to start to form rolled structures. In a few areas, fibres

were found, as well as smaller, prolate particles. At 1  $\mu\text{M}$ , these prolate particles dominated, with lengths of  $41 \pm 8$  nm and widths of  $19 \pm 3$  nm. These observations indicate that as the concentration is raised, the prolate ‘seeds’ merge to form lamellae, which then roll to give fibres. This matches up with the DLS and NR data indicating a structure/concentration relationship. The measured dimensions indicate that the polymer chains adopt compact rather than extended conformations, since their stretched length would be  $\sim 38$  nm. Since these samples were made by dilution, it is important to note that the assemblies must have a degree of dynamism, allowing the fibres to break down into lamellae and seeds. Contrastingly, in the same buffer at 100  $\mu\text{M}$  the sequence-isomer **(C12-HEG)<sub>10</sub>** produced only very few irregular aggregates, consistent in size with the DLS observations. We attribute this to the sample consisting of random coils which can aggregate through occasional patches of increased hydrophobicity (Fig 3b, S9).

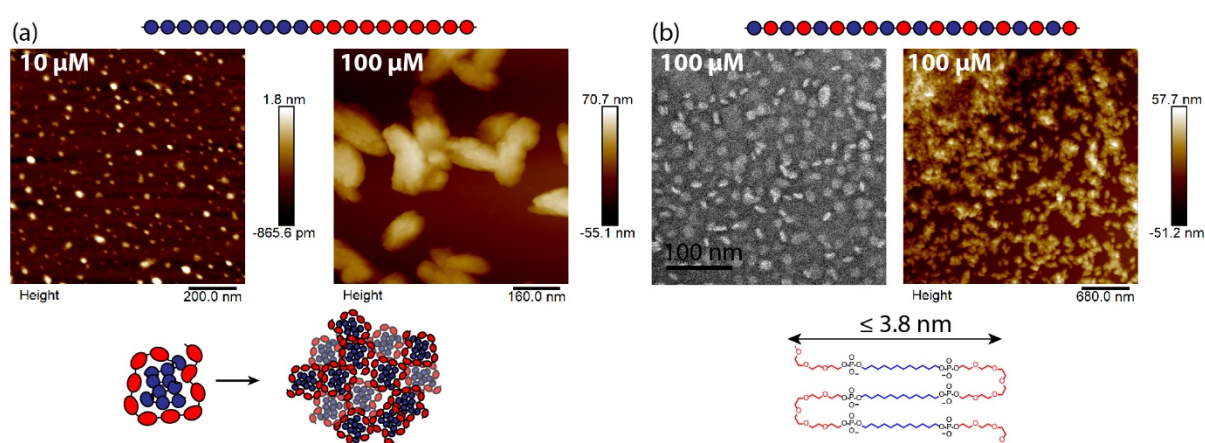


**Figure 4.** Self-assembly in TAMg buffer of (a) **C12<sub>10</sub>-HEG<sub>10</sub>** and (b) **(C12-HEG)<sub>10</sub>**.

In TAMg buffer, the results were quite different. **C12<sub>10</sub>-HEG<sub>10</sub>** at 100  $\mu\text{M}$  was observed by TEM to consist of prolate particles smaller ( $18 \pm 4$  nm length  $\times$   $7 \pm 1$  nm diameter) than those seen in TBE at 1  $\mu\text{M}$  (Fig. S10). This is consistent with the doubly charged cations promoting tight collapse of the polymers, similar to compaction of DNA by metal cations.<sup>31</sup> The higher resolution provided by AFM (Fig. 4a, S13) showed these structures to be somewhat ‘lumpy.’ Upon dilution, no objects could be observed by TEM, but AFM revealed a surface covered by many spherical particles with average heights of  $1.3 \pm 0.6$  nm and diameters of  $22.5 \pm 8.5$  nm (Fig 4a, S14). Taking tip convolution into account, these measurements are consistent with formation of SCNPs. The lumpiness of the structures formed at 100  $\mu\text{M}$  may be indicative of their structure consisting of aggregates of these SCNPs. With **(C12-HEG)<sub>10</sub>**, at 100  $\mu\text{M}$  both fluid lamellar and discoid structures were seen by TEM (Fig. 4b, S11) with average heights of  $6.1 \pm 1.0$  nm and diameters of  $14.6 \pm 3.2$  nm. The discs were confirmed by AFM (Fig. 4b, S15) with average heights of  $29.0 \pm 9.6$  nm and diameters of  $100 \pm 73$  nm for the discs at 100  $\mu\text{M}$ . It is not clear at this stage how ordered structures of that size range could be assembled from the alternating polymer since the smallest dimension of the particles is much larger than the maximum possible distance obtained by the polymer adopting a concertina conformation ( $\sim 3.8$  nm), as is seen in other self-assembling alternating polymers.<sup>32</sup> It may be that  $\text{Mg}^{2+}$  induces crystallisation, but deeper investigation will be required to assess that.

**Table 1.** Summary of self-assembly by sequence, buffer, and concentration.

Buffer	C12 <sub>10</sub> -HEG <sub>10</sub>		(C12-HEG) <sub>10</sub>	
	TBE	TAMg	TBE	TAMg
100 $\mu$ M	Rolls	Lumpy particles	Random aggregates	Discs and film
10 $\mu$ M	Lamellae	SCNPs	Random coil	Film
1 $\mu$ M	Seeds	-	-	-

In summary, we have for the first time synthesised perfectly uniform, non-biological, sequence-defined polymers which display self-assembly directly attributable to sequence (Table 1). The level of patterning explored here is at its simplest but the combination of macromolecular length and level of synthetic precision here is unique. Even these simple patterns have resulted not just in the production of unusual nanostructures, going beyond the classical star micelle/worm/vesicle schema, but also show interesting effects of dynamism not usually found in self-assembled polymer systems; in fact the outcomes have been far more interesting than our initial hypotheses anticipated (*vide supra*). This is a strength of the charged phosphate group, which has allowed us to produce these nanostructures by direct dissolution, rather than a solvent switch, and also led to salt-driven structural switching. These findings raise interesting prospects for interface with biology, in which the ability to alter nanostructures based on the specific environment could be used to develop new diagnostics, drug carriers, or therapeutic systems themselves. We are working to diversify our monomer pool and develop methods to analyse self-assembly in a high-throughput manner to fully exploit the potential of the phosphoramidite method in development of next-generation materials.

### Supporting Information

Synthetic and analytical protocols, and supplementary DLS, fluorescence, TEM and AFM data are available in the Supporting Information document.

### Author ORCIDs

Nadeema Appukutti: 0000-0002-6848-212

Christopher J. Serpell: 0000-0002-2848-9077

### Acknowledgements

The authors are grateful to the University of Kent for a funding and for a Vice-Chancellor's Scholarship.

### References

- 1 J.-F. Lutz, M. Ouchi, D. R. Liu and M. Sawamoto, Sequence-Controlled Polymers, *Science*, 2013, **341**, 1238149–1238149.
- 2 J.-F. Lutz, J.-M. Lehn, E. W. Meijer and K. Matyjaszewski, From precision polymers to complex materials and systems, *Nat. Rev. Mater.*, 2016, **1**, 16024.
- 3 M. A. R. Meier and C. Barner-Kowollik, A New Class of Materials: Sequence-Defined Macromolecules and Their Emerging Applications, *Adv. Mater.*, 2019, 1806027.
- 4 M. R. Golder, Y. Jiang, P. E. Teichen, H. V.-T. Nguyen, W. Wang, N. Milos, S. A. Freedman, A. P. Willard and J. A. Johnson, Stereochemical Sequence Dictates Unimolecular Diblock Copolymer Assembly, *J. Am. Chem. Soc.*, 2018, **140**, 1596–1599.
- 5 W. Zhang, W. Shan, S. Zhang, Y. Liu, H. Su, J. Luo, Y. Xia, T. Li, C. Wesdemiotis, T. Liu, H. Cui, Y.

- Li and S. Z. D. Cheng, Sequence isomeric giant surfactants with distinct self-assembly behaviors in solution †, *Chem. Commun*, 2019, **55**, 636.
- 6 C. K. Lyon, A. Prasher, A. M. Hanlon, B. T. Tuten, C. A. Tooley, P. G. Frank and E. B. Berda, A brief user's guide to single-chain nanoparticles, *Polym. Chem.*, 2015, **6**, 181–197.
- 7 A. M. Hanlon, C. K. Lyon and E. B. Berda, What Is Next in Single-Chain Nanoparticles?, *Macromolecules*, 2016, **49**, 2–14.
- 8 X. Li, T. Qi, K. Srinivas, S. Massip, V. Maurizot and I. Huc, Synthesis and Multibromination of Nanosized Helical Aromatic Amide Foldamers via Segment-Doubling Condensation, *Org. Lett.*, 2016, **18**, 1044–1047.
- 9 H. K. Murnen, A. R. Khokhlov, P. G. Khalatur, R. A. Segalman and R. N. Zuckermann, Impact of Hydrophobic Sequence Patterning on the Coil-to-Globule Transition of Protein-like Polymers, *Macromolecules*, 2012, **45**, 5229–5236.
- 10 Z. Lockhart and P. C. Knipe, Conformationally Programmable Chiral Foldamers with Compact and Extended Domains Controlled by Monomer Structure, *Angew. Chemie Int. Ed.*, 2018, **57**, 8478–8482.
- 11 M. H. Caruthers, Chemical Synthesis of DNA and DNA Analogues, *Acc. Chem. Res.*, 1991, **24**, 278–284.
- 12 T. G. W. Edwardson, K. M. M. Carneiro, C. J. Serpell and H. F. Sleiman, An efficient and modular route to sequence-defined polymers appended to DNA, *Angew. Chemie - Int. Ed.*, 2014, **53**, 4567–4571.
- 13 C. J. Serpell, T. G. W. Edwardson, P. Chidchob, K. M. M. Carneiro and H. F. Sleiman, Precision polymers and 3D DNA nanostructures: Emergent assemblies from new parameter space, *J. Am. Chem. Soc.*, 2014, **136**, 15767–15774.
- 14 P. Chidchob, T. G. W. Edwardson, C. J. Serpell and H. F. Sleiman, Synergy of Two Assembly Languages in DNA Nanostructures: Self-Assembly of Sequence-Defined Polymers on DNA Cages, *J. Am. Chem. Soc.*, 2016, **138**, 4416–4425.
- 15 D. Bousmail, L. Amrein, J. J. Fakhoury, H. H. Fakih, J. C. C. Hsu, L. Panasci and H. F. Sleiman, Precision spherical nucleic acids for delivery of anticancer drugs, *Chem. Sci.*, 2017, **8**, 6218–6229.
- 16 D. de Rochambeau, M. Barłóg, T. G. W. Edwardson, J. J. Fakhoury, R. S. Stein, H. S. Bazzi and H. F. Sleiman, 'DNA–Teflon' sequence-controlled polymers, *Polym. Chem.*, 2016, **7**, 4998–5003.
- 17 A. Al Ouahabi, L. Charles and J.-F. Lutz, Synthesis of Non-Natural Sequence-Encoded Polymers Using Phosphoramidite Chemistry, *J. Am. Chem. Soc.*, 2015, **137**, 5629–5635.
- 18 A. Al Ouahabi, M. Kotera, L. Charles and J.-F. Lutz, Synthesis of Monodisperse Sequence-Coded Polymers with Chain Lengths above DP100, *ACS Macro Lett.*, 2015, **4**, 1077–1080.
- 19 G. Cavallo, A. Al Ouahabi, L. Oswald, L. Charles and J.-F. Lutz, Orthogonal Synthesis of 'easy-to-Read' Information-Containing Polymers Using Phosphoramidite and Radical Coupling Steps, *J. Am. Chem. Soc.*, 2016, **138**, 9417–9420.
- 20 R. Häner, F. Garo, D. Wenger and V. L. Malinovskii, Oligopyrenotides: Abiotic, Polyanionic Oligomers with Nucleic Acid-like Structural Properties, *J. Am. Chem. Soc.*, 2010, **132**, 7466–7471.

- 21 V. L. Malinovskii, A. L. Nussbaumer and R. Häner, Oligopyrenotides: Chiral Nanoscale Templates for Chromophore Assembly, *Angew. Chemie Int. Ed.*, 2012, **51**, 4905–4908.
- 22 M. Vybornyi, A. Rudnev and R. Häner, Assembly of Extra-Large Nanosheets by Supramolecular Polymerization of Amphiphilic Pyrene Oligomers in Aqueous Solution, *Chem. Mater.*, 2015, **27**, 1426–1431.
- 23 S. Rothenbühler, C. D. Bösch, S. M. Langenegger, S.-X. Liu and R. Häner, Self-assembly of a redox-active bolaamphiphile into supramolecular vesicles, *Org. Biomol. Chem.*, 2018, **16**, 6886–6889.
- 24 F. Westheimer, Why nature chose phosphates, *Science*, 1987, **235**, 1173–1178.
- 25 T. Steinbach and F. R. Wurm, Poly(phosphoester)s: A New Platform for Degradable Polymers, *Angew. Chemie Int. Ed.*, 2015, **54**, 6098–6108.
- 26 K. N. Bauer, H. T. Tee, M. M. Velencoso and F. R. Wurm, *Prog. Polym. Sci.*, 2017, **73**, 61–122.
- 27 N. Appukutti and C. J. Serpell, High definition polyphosphoesters: between nucleic acids and plastics, *Polym. Chem.*, 2018, **9**, 2210–2226.
- 28 V. T. Ravikumar, R. K. Kumar, P. Olsen, M. N. Moore, R. L. Carty, M. Andrade, D. Gorman, X. Zhu, I. Cedillo, Z. Wang, L. Mendez, A. N. Scozzari, G. Aguirre, R. Somanathan and S. Berneès, UnyLinker: An Efficient and Scaleable Synthesis of Oligonucleotides Utilizing a Universal Linker Molecule: A Novel Approach To Enhance the Purity of Drugs, *Org. Process Res. Dev.*, 2008, **12**, 399–410.
- 29 P. Greenspan, E. P. Mayer and S. D. Fowler, Nile red: A selective fluorescent stain for intracellular lipid droplets, *J. Cell Biol.*, 1985, **100**, 965–973.
- 30 P. Greenspan and S. D. Fowler, Spectrofluorometric studies of the lipid probe, Nile Red, *J. Lipid Res.*, 1985, **26**, 781–789.
- 31 A. Estévez-Torres and D. Baigl, DNA compaction: fundamentals and applications, *Soft Matter*, 2011, **7**, 6746.
- 32 Q. Xu, S. Li, C. Yu and Y. Zhou, Self-assembly of Amphiphilic Alternating Copolymers, *Chem. - A Eur. J.*, , DOI:10.1002/chem.201804067.